Nat. Hazards Earth Syst. Sci. Discuss., 2, 1465–1479, 2014
www.nat-hazards-earth-syst-sci-discuss.net/2/1465/2014/
doi:10.5194/nhessd-2-1465-2014

Natural Hazards
and Earth System
Sciences
Discussions
Open Access

Brief communication: Rapid mapping of event landslides: the 3 December 2013 Montescaglioso landslide (Italy)

A. Manconi[1], F. Casu[2], F. Ardizzone[3], M. Bonano[2], M. Cardinali[3], C. De Luca[2], E. Gueguen[4], I. Marchesini[3], M. Parise[5], C. Vennari[5], R. Lanari[2], and F. Guzzetti[3]

[1]CNR IRPI, Strada delle Cacce 73, 10135, Torino, Italy
[2]CNR IREA, Via Diocleziano 328, 80124 Napoli, Italy
[3]CNR IRPI, Via della Madonna Alta 126, 06128 Perugia, Italy
[4]CNR IMAA, C.da Santa Loja, Tito Scalo, 85050 Potenza, Italy
[5]CNR IRPI, Via Amendola, 122/I, 70126 Bari, Italy

Received: 31 January 2014 – Accepted: 5 February 2014 – Published: 14 February 2014

Correspondence to: A. Manconi (andrea.manconi@irpi.cnr.it)

Published by Copernicus Publications on behalf of the European Geosciences Union.

Abstract

We present a new approach for the rapid measurement of the three-dimensional surface deformations caused by a large, rapid moving landslide, in an emergency scenario. The technique exploits the amplitude information of high spatial and temporal resolution Synthetic Aperture Radar images captured by the COSMO-SkyMed satellites immediately before and after the landslide event. We show the results obtained for the Montescaglioso landslide, southern Italy, a large and rapid slope failure triggered by prolonged and intense rainfall on 3 December 2013. The slope failure damaged a main road, private homes, and commercial buildings. The results of our work open to the possibility of preparing accurate surface deformation maps for large, rapid moving landslides.

1 Introduction

Large landslides occur in several regions of the Earth, causing local damage and casualties (Petley, 2012). In places, these phenomena affect urban areas, buildings, roads and rails, threatening the population and causing emergency situations. In such scenarios, rapid mapping of the location and extent of the surface deformation caused by landslides provides important hints for the rapid response of civil protection authorities, for rescue and recovery operations, as well as to design and deploy effective monitoring systems. Usually, post-event landslide maps are compiled through field mapping, and/or the visual analysis of aerial photographs taken shortly after the landslide event (Guzzetti et al., 2012). Where the ground displacements are in the order of several meters, and the velocity of the failure is rapid to very rapid (Cruden and Varnes, 1996), access to the landslide area may be difficult or impossible, or too dangerous to perform field mapping. Also, post-event aerial photography of adequate resolution may not be available. In these circumstances, remote sensing techniques provide an effective alternative to perform semi-quantitative or quantitative assessments of the extent and the amount of the ground deformations. Among several remote sensing techniques, space-borne Synthetic Aperture Radar (SAR) has demonstrated its efficiency to monitor changes on the Earth's surface produced by natural and human induced processes (Rott, 2009). In particular, Differential SAR Interferometry (DInSAR) allows measuring ground deformation by properly analysing the phase difference between two SAR images (Massonnet et al., 1993) acquired over the same area at different times and from different orbital positions (hereafter referred to as temporal and spatial baselines, respectively). The main advantage of DInSAR is the possibility to generate surface deformation and velocity maps covering large to very large areas (10^2–10^5 km^2), with sub-centimetric measurement accuracy. A known limitation of DInSAR consists in the fact that accurate measurements of the deformation cannot be performed where the deformation is rapid or large. In such cases, the interferometry phase information may be affected by high fringe rates leading to processing difficulties in the phase unwrapping step and/or to coherence loss due to misregistration errors (Casu et al., 2011). However, if the deformation introduces geometric distortions without significantly affecting the SAR image reflectivity, displacements can be observed in the amplitudes of the SAR image pairs acquired before and after the event. Although measurement accuracies gained with this approach, hereinafter referred to as "pixel-offset" (PO), are significantly lower than those obtained by DInSAR (Casu et al., 2011), the PO approach has the advantage of providing 2-D displacement information i.e., the components across and along the satellite's track (range and azimuth directions, respectively). Moreover, considering PO analyses for SAR images captured along ascending and descending orbits on the same area, it is possible to retrieve the full three-dimensional deformation field (Ayele et al., 2009; Raucoules et al., 2013).

In this work, we present the first results of a rapid mapping effort conducted during a recent landslide emergency occurred in December 2013 in the Montescaglioso municipality, Basilicata Region, southern Italy. In the following, we first describe the main features of the new landslide. Then, we present qualitative and semi-quantitative information obtained immediately after the event using consolidated mapping approaches

(Guzzetti et al., 2012). Next, we show the results of a three-dimensional surface deformation map obtained using the PO technique applied to high resolution SAR images acquired by the COSMO-SkyMed (CSK) satellites before and after the landslide event.

2 Local setting

On 3 December 2013, a large landslide struck SW of Montescaglioso, a town located in the Matera Province, southern Italy (Fig. 1). As many towns in Southern Italy, the inhabited area is located at the top of a hill bounded by steep slopes, showing widespread development of landslides of different typologies. In particular, the slope affected by the new landslide is characterized by several morphologies related to ancient gravitational movements, as also reported in the official geological map, produced during the 1950's, where extensive landslide bodies were mapped. Mean annual rainfall in the area is 570 mm, with the highest monthly value typically occurring in November (187 mm).

In the general area crop out sediments of the "Bradanic Trough", Pleistocene in age (Tropeano et al., 2002), including a regression (coarsening upward) sequence made up of clay (at the bottom), sand, and gravel (at the top). In the slope where the new Montescaglioso landslide occurred, sediments are heterogeneous, as demonstrated by the presence of large blocks of conglomerates (max size about 5 m × 3 m) found at different elevations in the slope. We attribute the chaotic distribution of the materials to repeated, old and very old landslides, the result of a complex morphological evolution of the area.

3 The new Montescaglioso landslide

The new Montescaglioso landslide occurred after 56 h of continuous rainfall, from 30 November (14:00 CET) to 2 December (22:00 CET), with a cumulated rainfall measured at the Ginosa rain gauge, located 8 km from Montescaglioso, of $E = 151.6$ mm,

Title Page
Abstract Introduction
Conclusions References
Tables Figures
◀| |▶
◀ ▶
Back Close
Full Screen / Esc
Printer-friendly Version
Interactive Discussion

and mean rainfall intensity $I = 2.7\,\mathrm{mm\,h^{-1}}$. Two months before the landslide event, between 5 and 8 October 2013, the general area between Apulia and Basilicata, including the town of Montescaglioso, was struck by a heavy rainfall event with a cumulated rainfall $E = 246\,\mathrm{mm}$, and a mean rainfall intensity $I = 3.6\,\mathrm{mm\,h^{-1}}$. The event caused widespread flooding, numerous shallow landslides, severe economic losses, and four fatalities.

The length of the landslide deposits, measured along its main axis, is $L_\mathrm{L} \sim 1.2 \times 10^3\,\mathrm{m}$, and the width, measured perpendicularly to its main axis, is $W_\mathrm{L} \sim 8.0 \times 10^2\,\mathrm{m}$. The landslide extended from ca. 200 m of elevation in the source area to ca. 110 m of elevation at the toe, and affected a total area $A_\mathrm{L} \sim 3.0 \times 10^5\,\mathrm{m}^2$. The slope failure damaged the freeway connecting the town of Montescaglioso to the Province road SP175, disrupting more than 500 m of the road. The failure also involved a few warehouses, a supermarket, and private homes located on the right bank of a channel in the area known as “Cinque Bocche” (Fig. 1). Anecdotal information collected immediately after the event indicates that the landslide was rapid, with the main movement occurring in a short period of 15–20 min. The movement started at 13:05 CET, and affected the freeway shortly afterward. Next, the movement involved the lower-left flank of the landslide, resulting in the formation of a swarm of scarps and counterscarps, several tens of meters in length and with a maximum height of seven to eight meters, damaging several buildings. A house (shown by “C” in Fig. 1) was moved a few meters downslope and tilted, fortunately retaining its overall integrity and allowing the inhabitants to escape avoiding direct consequences.

4 Geomorphological mapping of the new Montescaglioso landslide

To respond to a request of the Italian National Department for Civil Protection (DPC), in the period from 9 to 24 December 2013 we conducted an initial geomorphological analysis to prepare a preliminary landslide inventory map and characterize the new Montescaglioso event in the broader context of the pre-existing landslides in the study area. This was done through the visual interpretation of seven sets of black-and-white stereoscopic aerial photographs taken from 1947 to 2003, at scales ranging from 1 : 24 000 to 1 : 36 000. The aerial photographs were obtained at low resolution from the online catalogue of aerial photographs of the Istituto Geografico Militare Italiano (IGMI, http://www.igmi.org/voli/). Despite the low resolution of the aerial photographs, visual inspection of the photographs allowed to identify and map a large number of geomorphological features related to the presence of pre-existing mass movements. In particular, the geomorphological landslide map shows (Fig. S1 in Supplement): (i) a large, very old landslide, largely dismantled by erosion processes, including other landslides, that affected the entire slope, (ii) a number of smaller and more recent landslides, mainly translational slides and flows, which are distributed within and at the edges of the pre-existing, very old landslide, and (iii) numerous, mostly minor, landslide escarpments. Inside the pre-existing very old phenomenon it was possible to recognize different generations of landslides. Some of these landslides intersect the town of Montescaglioso (Fig. S1 in Supplement).

In addition to the interpretation of the aerial photographs, we performed field surveys to evaluate the main consequences of the landslide, and to compile a map of the surface deformation in the landslide area. The field surveys were aided by the visual analysis of post-event terrestrial photographs, and photographs taken during helicopter flights (Fig. S2 in Supplement). The geomorphological features mapped in the field and through the inspection of the terrestrial and the helicopter photographs included single fractures, sets of fractures, tension cracks, trenches up to 6 m in depth/width, and pressure ridges. Many of the geomorphological features mapped immediately after the landslide event were later destroyed by the construction of temporary roads.

5 Three-dimensional surface deformation from space-borne SAR

The Italian Space Agency (ASI) made available a set of X-band CSK images for the study area. The dataset consists of 31 images taken along ascending orbits over the

30 January 2012–18 December 2013 time interval, and 12 images taken along descending orbits over the period from 21 March 2012 to 12 December 2013, both subsets including a single post-event image.

A first DInSAR analysis was performed on the acquisitions across the investigated event. However, in the area affected by the new Montescaglioso landslide the DInSAR processing produced unsatisfactory results, which were primarily attributed to the excessive fringe noise related to the fast-moving deformation pattern (Fig. S3 in Supplement). We note that the retrieved DInSAR signal is generally very noisy also in areas located near (but outside) the new Montescaglioso landslide. We consider this a consequence of the large temporal and/or spatial baselines that characterize the available CSK image pairs across the landslide event and, in general, the entire data distribution (Fig. S4 in Supplement).

Considering the poor quality of the DInSAR results, we applied the amplitude-based pixel-offset technique to the SAR data pairs across the event with the smallest spatial baselines, to reduce the impact of the spatial decorrelation. In particular, we considered the ascending 16 January 2013–18 December 2013, and the descending 10 January 2013–12 December 2013 data pairs, characterized by spatial baselines of 155 m and 40 m, respectively, and covering approximately the same time interval. As already outlined, the PO technique allows identifying with a good spatial detail the areas affected by large displacements, which are on the order or exceed the pixel size e.g., three meters for the available CSK data. By combining the PO measurements obtained from the CSK ascending and descending orbits, we determined the three-dimensional deformation pattern caused by the new Montescaglioso landslide. Inspection of Fig. 2 reveals that the ground displacements have a dominant SSW component, with values exceeding 10 m among large part of the landslide deposit and, in some cases, reaching about 20 m. Furthermore considerable subsidence values were identified in the areas experiencing the largest damages, while a distinct uplift (up to 5 m) was imaged close to the accumulation area.

6 Discussion and conclusions

Rapid mapping via remote sensing of human induced and/or natural disasters during emergency scenarios is becoming a standard practice to support emergency and recovery operations (Boccardo, 2013). This includes analyses of data acquired from different remote platforms (ground based systems, manned and unmanned aerial systems, and space-borne systems), and from different types of sensors (e.g., panchromatic, multispectral, hyperspectral, thermal, LiDAR, radar). For large, catastrophic landslides, selection of the most appropriate mapping and monitoring technique depends on multiple factors (Wieczorek and Snyder, 2009). After a new landslide event, the rapid evaluation of the area affected by the mass-wasting, as well as measurements of the associated surface deformation, are extremely important. Indeed, this information is crucial to have some guidance for the planning and installation of a monitoring network, and eventually of an early warning system aimed at ensuring safety for people and infrastructures. Moreover, post-event deformation maps represent the base of knowledge to assess further geomorphological analyses and geophysical investigations, as well as for the evaluation of the residual risk and thus for the design and realization of mitigation and stabilization measures (Revellino et al., 2010).

In general, aerial and satellite optical images acquired before and after a landslide event are considered for first order evaluations of ground displacements in emergency scenarios; however, optical data can usually provide qualitative and/or semi quantitative bi-dimensional information only. Furthermore, the availability of exploitable data strictly depends on the meteorological conditions at the acquisition time, as for example cloud coverage might compromise the visibility of the area of interest. Airborne LiDAR associated with photogrammetric surveys represent also a powerful remote sensing methodology to map post-event landslide deformation, as well as to estimate the mobilized mass volume (e.g., Giordan et al., 2013). Further, the acquisition of LiDAR data might be in some cases hampered by the high costs and operational issues, as well as by unsuitable meteorological conditions.

Title Page
Abstract | Introduction
Conclusions | References
Tables | Figures
◀| |▶
◀ ▶
Back | Close
Full Screen / Esc
Printer-friendly Version
Interactive Discussion

When the slope exposure is suitable with the satellite acquisition geometry (Colesanti and Wasowski, 2006), space-borne SAR can be considered as a valid alternative to map and measure surface deformation relevant to landslide phenomena. This technique has the main advantage to acquire data day and night, as well as in any weather condition. Though, as mentioned in the introduction, the exploitation of DInSAR technique in large and catastrophic landslide scenarios is hindered by the large and/or rapid deformation usually associated with this kind of events. On the other hand, in this work we have shown how the amplitude information contained in space-borne SAR images can be exploited to map and measure rapid deformation caused by large landslides. We applied the PO technique by considering SAR image pairs acquired before and after the new Montescaglioso landslide by the CSK constellation, which ensures high spatial resolution (pixel 3 m × 3 m) and short revisit times (16 days on average for the available datasets). In addition, we combined the PO results obtained from ascending and descending orbits to retrieve three-dimensional ground displacements. To our knowledge, this is the first time that this approach has been applied to provide rapid mapping of the three-dimensional surface displacements in a landslide emergency scenario.

The combination of rapid geomorphological mapping, rapid field mapping, and rapid measurements of three-dimensional deformation herein presented has been crucial to support DPC operations during the first emergency phases. The results of the geomorphological multi-temporal analysis allowed to recognize the presence of landslides of sizes, shapes, and relative age that are different and affect larger portions than those identified in the existing official documents and maps. The field mapping effort performed shortly after the event allowed to retrieve useful insights for understanding the kinematics of the landslide, and for the reconstruction of the geometry of slip surfaces (Parise, 2003). Two major landslide scarps were identified: the first, located in the middle slope and involving the hypermarket area, which should correspond to the first phase of the event, while the second, located closer to the slope divide, was presumably generated during the second phase, and likely resulted from the retrogressive evolution of the entire phenomenon. Also the 3-D ground deformation measurements (retrieved through the PO analysis) allowed imaging the presence of two main directions of motion, one associated with the main landslide event (SSW) and a secondary smaller event (SSE), respectively (see Fig. 3). Thus, PO results are well in agreement with both the magnitude and the deformation mechanisms recognized and mapped during field observations. The joint interpretation of the results obtained with classical and new methods presented in this work has been essential for the design of the topographic monitoring network installed in the Montescaglioso area, as well as for the mitigation strategies that will be implemented.

Finally, we remark that future integrations of the information gained from classical geomorphological analyses and SAR images, through DInSAR and/or PO techniques, might open a new scenario for the analysis of landslide phenomena presenting complex spatial and/or temporal heterogeneities of the deformation field. Moreover, the increasing availability of space-borne high spatial and/or temporal resolution SAR images from satellites ensuring a relatively short revisit times, such as COSMO-SkyMed, TerraSAR-X, as well as the forthcoming ALOS PALSAR-2 and Sentinel missions, will further enhance the possibility to achieve rapid mapping of large landslides in complex emergency scenarios, and thus support civil protection operations in the event's aftermath.

Supplementary material related to this article is available online at http://www.nat-hazards-earth-syst-sci-discuss.net/2/1465/2014/nhessd-2-1465-2014-supplement.pdf.

Acknowledgements. Research funded by the National Department of Civil Protection (DPC). The Italian Space Agency (ASI) provided the COSMO-SkyMed images used in this study. We are grateful to L. Candela (ASI) for CSK data provisioning.

References

Allasia, P., Manconi, A., Giordan, D., Baldo, M., and Lollino, G.: ADVICE: a new approach for near-real-time monitoring of surface displacements in landslide hazard scenarios, Sensors, 13, 8285–8302, doi:10.3390/s130708285, 2013.

Ayele, A., Keir, D., Ebinger, C., Wright, T. J., Stuart, G. W., Buck, W. R., Jacques, E., Ogubazghi, G., and Sholan, J.: September 2005 mega-dike emplacement in the Manda-Harraro nascent oceanic rift (Afar depression), Geophys. Res. Lett., 36, L20306, doi:10.1029/2009GL039605, 2009.

Boccardo, P.: New perspectives in emergency mapping, Eur. J. Remote Sens., 46, 571–582, doi:10.5721/EuJRS20134633, 2013.

Casu, F., Manconi, A., Pepe, A., and Lanari, R.: Deformation time-series generation in areas characterized by large displacement dynamics: the SAR amplitude pixel-offset SBAS technique, IEEE T. Geosci. Remote, 49, 2752–2763, doi:10.1109/TGRS.2010.2104325, 2011.

Colesanti, C. and Wasowski, J.: Investigating landslides with space-borne Synthetic Aperture Radar (SAR) interferometry, Eng. Geol., 88), 173–199, doi:10.1016/j.enggeo.2006.09.013, 2006.

Cruden, D. M. and Varnes, D. J.: Landslides Types and Processes, in: Turner, A. K. and Schuster, R. L., Landslides: Investigation and Mitigation. Transportation Research Board Special Report 247, National Academy Press, WA, 36–75, 1996.

Giordan, D., Allasia, P., Manconi, A., Baldo, M., Santangelo, M., Cardinali, M., Corazza, A., Albanese, V., Lollino, G., and Guzzetti, F.: Morphological and kinematic evolution of a large earthflow: the Montaguto landslide, southern Italy, Geomorphology, 187, 61–79, doi:10.1016/j.geomorph.2012.12.035, 2013.

Guzzetti, F., Mondini, A. C., Cardinali, M., Fiorucci, F., Santangelo, M., and Chang, K.-T.: Landslide inventory maps: new tools for an old problem, Earth-Sci. Rev., 112, 42–66, doi:10.1016/j.earscirev.2012.02.001, 2012.

Massonnet, D., Rossi, M., Carmona, C., Adragna, F., Peltzer, G., Feigl, K., and Rabaute, T.: The displacement field of the Landers earthquake mapped by radar interferometry, Nature, 364, 138–142, doi:10.1038/364138a0, 1993.

Parise, M.: Observation of surface features on an active landslide, and implications for understanding its history of movement, Nat. Hazards Earth Syst. Sci., 3, 569–580, doi:10.5194/nhess-3-569-2003, 2003.

Petley, D.: Global patterns of loss of life from landslides, Geology, 40, 927–930, doi:10.1130/G33217.1, 2012.

Raucoules, D., de Michele, M., Malet, J.-P., and Ulrich, P.: Time-variable 3D ground displacements from high-resolution synthetic aperture radar (SAR). Application to La Valette landslide (South French Alps), Remote Sens. Environ., 139, 198–204, doi:10.1016/j.rse.2013.08.006, 2013.

Revellino, P., Grelle, G., Donnarumma, A., and Guadagno, F. M.: Structurally controlled earth flows of the Benevento province (southern Italy), B. Eng. Geol. Environ., 69, 487–500, doi:10.1007/s10064-010-0288-9, 2010.

Rosen, P. A., Hensley, S., Peltzer, G., and Simons, M.: Updated repeat orbit interferometry package released, Eos T. Am. Geophys. Un., 85, 47–47, doi:10.1029/2004EO050004, 2004.

Rott, H.: Advances in interferometric synthetic aperture radar (InSAR) in earth system science, Prog. Phys. Geog., 33, 769–791, doi:10.1177/0309133309350263, 2009.

Tropeano, M., Sabato, L., and Pieri, P.: Filling and cannibalization of a foredeep: the Bradanic Trough, southern Italy, Geol. Soc. Lond. Spec. Publ., 191, 55–79, doi:10.1144/GSL.SP.2002.191.01.05, 2002.

Wieczorek, G. F. and Snyder, J. B.: Monitoring slope movements, in: Geological Monitoring: Boulder, Colorado, Geological Society of America, edited by: Young, R. and Norby, L., 245–271, 2009.

Title Page
Abstract Introduction
Conclusions References
Tables Figures
◀| |▶
◀ ▶
Back Close
Full Screen / Esc
Printer-friendly Version
Interactive Discussion

Title Page
Abstract
Introduction
Conclusions
References
Tables
Figures
◀I
▶I
◀
▶
Back
Close
Full Screen / Esc
Printer-friendly Version
Interactive Discussion

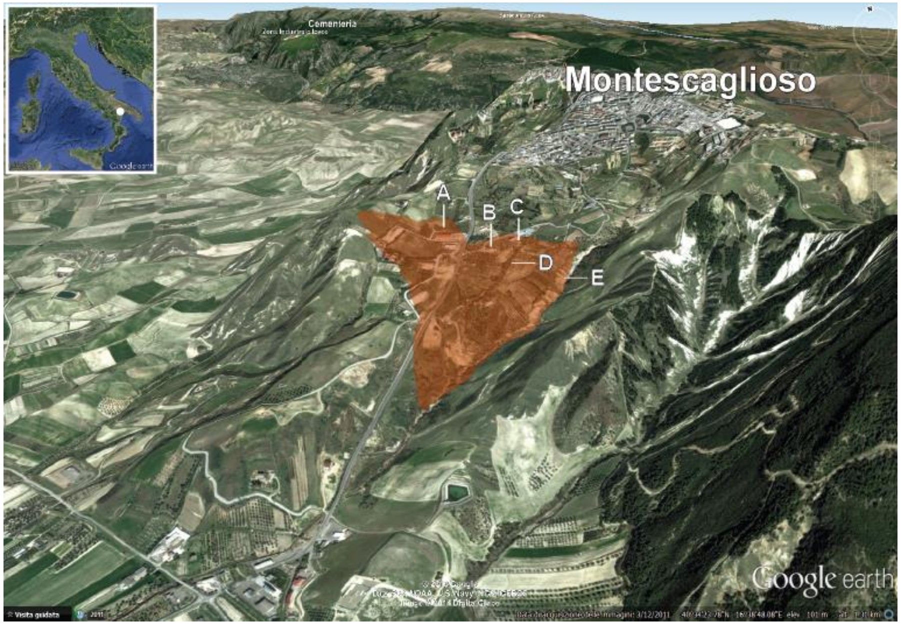

Fig. 1. Montescaglioso, southern Italy. The reddish area identifies qualitatively the area affected by mass wasting. The locations of the supermarket (A), as well as of the most damaged buildings (B and C) is also identified. Base map source: Google Earth™.

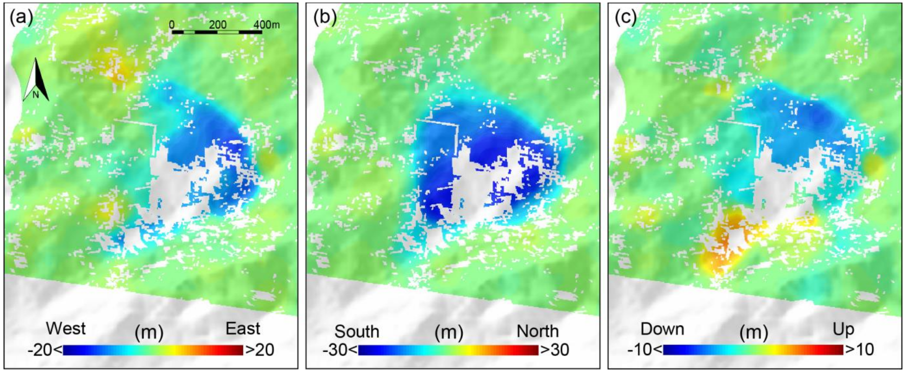

Fig. 2. The new Montescaglioso landslide. Pixel-offset results for the **(a)** East–West, **(b)** North–South, and **(c)** Up–Down components of the surface deformation obtained combining PO results obtained processing COSMO-SkyMed images acquired along ascending and descending orbits. In particular, we exploited the AMPCOR Fortran routine available in the ROI_PAC software (Rosen et al., 2004) using a matching window of 64 × 64 pixels. We calculated the PO considering a sparse grid with an under-sampling factor of four pixels. We applied a spatial smoothing filter to reduce high-frequency noise.

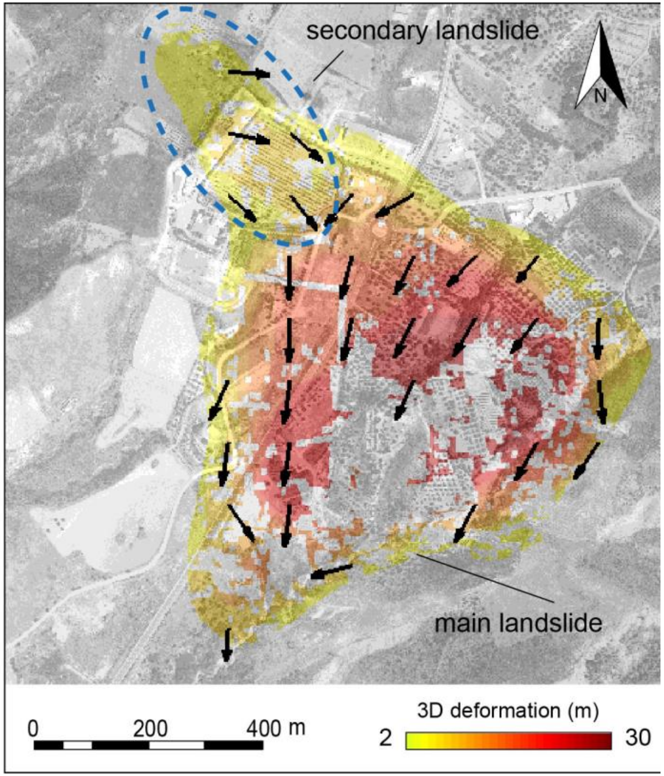

Fig. 3. The new Montescaglioso landslide. Map of the surface deformation map obtained via the PO analysis has been prepared using the ©3DA approach (Allasia et al., 2013). Colour scale shows magnitude of the three-dimensional deformation field. Arrows show the direction of movement (unit vectors), derived from the PO analysis, in the EW–NS plane. Deformations smaller than two meters are not shown. The deformation field shows two main directions of motion: (i) a dominant SSW direction caused by the main landslide, and (ii) a secondary SSE direction caused by a parasitic landslide, encompassed by the dashed blue ellipse.

Title Page
Abstract
Introduction
Conclusions
References
Tables
Figures
◀I
▶I
◀
▶
Back
Close
Full Screen / Esc
Printer-friendly Version
Interactive Discussion